

## Toward achieving the quantum ground state of a gram-scale mirror oscillator

Thomas Corbitt,<sup>1</sup> Yanbei Chen,<sup>2</sup> Edith Innerhofer,<sup>1</sup> Helge Müller-Ebhardt,<sup>3</sup> David Ottaway,<sup>1</sup>  
 Henning Rehbein,<sup>3</sup> Daniel Sigg,<sup>4</sup> Stanley Whitcomb,<sup>5</sup> Christopher Wipf,<sup>1</sup> and Nergis Mavalvala<sup>1</sup>

<sup>1</sup>LIGO Laboratory, Massachusetts Institute of Technology, Cambridge, MA 02139, USA

<sup>2</sup>Max-Planck-Institut für Gravitationsphysik, Am Mühlenberg 1, 14476 Potsdam, Germany

<sup>3</sup>Max-Planck-Institut für Gravitationsphysik (Albert Einstein Institute), Callinstraße 38, 30167 Hannover, Germany

<sup>4</sup>LIGO Hanford Observatory, Route 10, Mile marker 2, Hanford, WA 99352, USA

<sup>5</sup>LIGO Laboratory, California Institute of Technology, Pasadena, CA 91125, USA

(Dated: May 26, 2019)

Observation of quantum mechanical effects in objects visible to the unaided eye has long been thought impossible due to the overwhelming effect of thermal excitations at room temperature. Recent proposals [1, 11, 12, 13] suggest that a nano- or micro-mechanical oscillator may exhibit quantum effects if optically cooled by viscous radiation pressure, despite the thermal agitation arising from its sti-mechanical attachment to the environment. Here we propose an optical trap that does not contribute thermal noise, unlike a sti-mechanical connection. We show how the radiation pressure from two laser beams can optically trap a free mass, and we demonstrate the technique experimentally with a 1 gram mirror. For the first time optical forces are seen to completely dominate the dynamics of a macroscopic object, allowing for larger reductions in temperature than was previously possible. The observed optical trap has a maximum eigenfrequency of 5 kHz and a Young's modulus of 1.2 TPa, 20% stiffer than diamond. This technique both generates extreme cooling, and mitigates the detrimental effect of thermal decoherence. The lowest effective temperature measured is 800 mK, a factor of 370 below ambient room temperature, limited by technical noise in our apparatus. Temperature reductions 10 orders of magnitude below ambient are within reach through experimentally realizable parameters, which will enable the 1 gram mirror to approach the ground state. In contrast to previous work, we also show how the dynamical lifetime of the state, in the presence of thermal decoherence, may be extended by up to 7 orders of magnitude for this system. The proposed technique should expose the quantum-classical boundary in the strikingly large regime of gram-scale objects with  $10^{22}$  atoms.

To measure quantum effects in an oscillator, it is desirable to place the oscillator in a low energy state, such that the number of quanta in the mode  $N = E/h_e$  is comparable to 1, where  $E$  is the energy of the mode and  $e$  is the resonant frequency. The motion of a macroscopic oscillator is typically driven by thermal fluctuations due to its mechanical coupling with the environment. One way to achieve an energy state with  $N \approx 1$  for an object with temperature  $T$ , whose thermal energy initially exceeds the quantum ground state energy ( $k_B T > h_e$ ), is to apply feedback forces to reduce the oscillator's motion. The motion of an oscillator of mass  $M$  and spring constant  $K$  at its resonant frequency  $e = \sqrt{K/M}$  is related to its effective (or noise) temperature  $T_e$  by

$$\frac{1}{2}K x_{rms}^2 = \frac{1}{2}k_B T_e ; \quad (1)$$

where  $k_B$  is Boltzmann's constant. Reduction of the root-mean-squared motion  $x_{rms}$  and hence  $T_e$  by use of an optical damping force, referred to as "cold damping," has been proposed [2, 4, 5, 6] and demonstrated [1, 7, 8, 9, 10, 11, 12, 13], although far from the quantum limit.

After a quantum state of the oscillator is prepared, this state must survive for more than one oscillation period, so that measurements may be performed to observe quantum superpositions in macroscopic objects. Decoherence { departure from an ideal coherent quantum superposition { due to interaction of the quantum system with its classically noisy (thermal) environment typically prevents us from observing quantum effects. The thermal decoherence time of the state is given by [2, 3]

$$= \frac{2}{e} \frac{k_B T_e}{h_e}^{-1} ; \quad (2)$$

where  $e$  is the damping constant of the oscillator. The average number of oscillations  $N$  before decoherence is

$$N = \frac{k_B T_e}{h_e} \frac{e}{e}^{-1} ; \quad (3)$$

Unless  $N$  exceeds unity, the evidence for quantum behavior is quickly buried under classical thermal noise. This ordinarily precludes large objects from exhibiting quantum effects, since  $e$  typically decreases for larger objects,

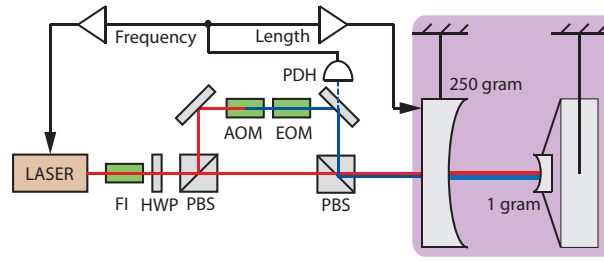


FIG. 1: Simplified schematic of the experiment. About 3 W of  $\lambda_0 = 1064$  nm Nd:YAG laser light passes through a Faraday isolator (FI) before it is split into two paths by a half-waveplate (HWP) and polarizing beam splitter (PBS) combination that allows control of the laser power in each path. The carrier (C) field comprises most of the light incident on the suspended cavity. About 5% of the light is frequency-shifted by one free spectral range (161.66 MHz) using an acousto-optic modulator (AOM), and phase modulated by an electro-optic modulator (EOM); this subcarrier (SC) field can further be detuned from resonance to create a second optical spring. The two beams are recombined on a second PBS before being injected into the cavity, which is mounted on a seismic isolation platform in a vacuum chamber (denoted by the shaded box). A Pound-Drever-Hall (PDH) error signal derived from the SC light reflected from the cavity is used to lock it, with feedback to both the cavity length as well as the laser frequency. By changing the frequency shift of the SC, the C can be shifted off resonance by arbitrarily large detunings. The high-power C beam is shown in red, while the low power SC beam is shown in blue.

due to their larger inertia. The commonly used cold damping technique has the effect of reducing the response of the oscillator at its resonance: this both reduces the temperature of the mode and increases its damping, thereby conserving  $N$ . Thus cold damping schemes are applicable only for nano- and micro-mechanical oscillators that initially satisfy  $N > 1$ . So far the fabrication of such systems remains an unsolved experimental challenge.

Here we propose a new technique that allows a system to exhibit quantum effects even though its initial configuration does not satisfy Eq. (3), opening the door for quantum effects to be observed in objects that are visible to the naked eye. Our scheme addresses two quantities of interest in measuring quantum states of macroscopic objects: (i) the average motion of the object ( $x_{ms}$  in Eq. 1), which is related to state preparation; and (ii) the number of oscillations of the mode before the state decays ( $N$  in Eq. 3), relating to state survival. This is achieved by using the radiation pressure forces from two laser beams to optically trap a mirror. In order to reduce thermal motion, the mirror must be as weakly coupled to the outside environment as possible, which in practice requires that the mirror should be suspended, with the stiffness of the suspension as soft as possible. One laser beam (the "carrier," denoted by C) is used to create a potential well by generating an optical restoring force, commonly known as an optical spring [9, 14, 15, 16, 17]. This potential well creates a mode of oscillation with a natural frequency of up to a few kilohertz. Unfortunately this mode is dynamically unstable because of the delayed optical response. An additional laser beam (the "subcarrier," denoted as SC) is used to stabilize the motion of the mirror within this potential well and to damp it to the ground state, similar to the aforementioned cold damping experiments. The advantage of this scheme is that the optical trap does not conserve  $N$ , because it changes the resonant frequency of the oscillator by orders of magnitude. This allows quantum effects to become visible in a system that would not otherwise show them.

The experiment shown schematically in Figure 1 was performed to demonstrate the optical trapping scheme. The input mirror of the  $L = 0.9$  m long cavity has mass of 0.25 kg and is suspended as a pendulum with oscillation frequency of 1 Hz for the longitudinal mode. The  $10^{-3}$  kg end mirror is suspended by two optical fibers 300  $\mu$ m in diameter, giving a natural frequency  $\omega_m = 2 \times 172$  Hz for the mechanical resonance. The input mirror transmissivity is  $T_1 = 800 \times 10^{-6}$ , while that of the end mirror is  $10^{-5}$ , and the laser wavelength is  $\lambda_0 = 1.064 \times 10^6$  m. When the round-trip cavity length is equal to an integer number of wavelengths of the laser light, the system becomes resonant and the intracavity power is enhanced relative to the incoming power by a resonant gain factor  $4 = T_1^{-1} \approx 5 \times 10^3$ , and with resonant linewidth (HWHM) of  $\Delta\nu = \frac{1}{4L} \approx 2 \times 11$  kHz. The stored power in the cavity exerts a constant (dc) radiation pressure force on each mirror.

If the resonance condition is exactly satisfied, the intracavity power depends quadratically on small changes in the length of the cavity. In this case the radiation pressure force is only a second order effect for the dynamics of the cavity. We assume that this constant radiation pressure force, as well as gravitational forces are balanced either naturally, or through external feedback forces (as in the experiment reported here). Consequently, only fluctuations of the radiation pressure force are considered. If the laser wavelength is detuned from the resonance condition, the intracavity power, and, therefore, the radiation pressure force, becomes linearly dependent on the length of the cavity,

analogous to a spring. The resulting spring constant is given in the frequency domain by [9, 17]

$$K(\omega) = \frac{\hbar \frac{1}{1 + (\omega/\omega_0)^2} (\omega/\omega_0)^2}{1 + (\omega/\omega_0)^2 (\omega/\omega_0)^2 + 4(\omega/\omega_0)^2} \quad (4)$$

$$K_0 = \frac{2 dP}{c dL} = \frac{128 I_0 (\omega_0)}{T_1^2 c_0} \frac{1}{1 + (\omega_0/\omega_0)^2}$$

where  $\omega_0$  is the frequency of the motion, and  $\omega_0$  and  $I_0$  are the detuning and input power of the laser, respectively. Note the dependence of  $K_0$  on  $\omega_0$ . For  $\omega_0 > 0$  (in our convention),  $K > 0$  corresponds to a restoring force, while  $\omega_0 < 0$  gives an anti-restoring force; we do not explore this regime experimentally since it is unstable (see Fig. 2). The light in the cavity responds to mirror motion on a time scale given by  $\tau_c^{-1}$ . This delay has two effects. First, for high frequency motion ( $\omega \gg \tau_c^{-1}$ ), the response of the cavity, and the corresponding radiation pressure force, are reduced, and we see from Eq. (4) that  $K(\omega) \approx K_0 (\omega_0/\omega)^2$ . Second, the response of the cavity lags the motion, leading to an additional force proportional to the velocity of the mirror motion (a viscous force with damping coefficient given by

$$B(\omega) = \frac{\hbar \frac{2K_0 M}{1 + (\omega/\omega_0)^2} (\omega/\omega_0)^2}{1 + (\omega/\omega_0)^2 (\omega/\omega_0)^2 + 4(\omega/\omega_0)^2}; \quad (5)$$

where  $M$  is the reduced mass of the two mirrors. It is this viscous force that the optical cooling schemes use to damp the thermal motion. The total radiation pressure force is  $F = Kx + M \dot{x}$  (i.e.  $\dot{x}$ ), where  $x$  is the fluctuation of the length of the cavity. Because the cavity response lags the motion of the mirrors, a restoring spring constant implies a negative damping. If both optical forces dominate their mechanical counterparts, then the system is unstable for any non-zero detuning, either due to an anti-restoring force, or an anti-damping force. In previous experiments, this has been counteracted through active feedback to stabilize the system [9].

The cold damping experiments previously proposed have only utilized the damping force to achieve cooling. In our scheme, we rely on the optical restoring force, as well as the damping force to achieve cooling. The advantage of this technique is that the natural resonant frequency of the system is shifted to

$$\omega_e = \frac{\omega_0}{\sqrt{\frac{2}{M} + K(\omega_e)M}}; \quad (6)$$

The shift of the resonant frequency directly modifies  $N$ , unlike the cold damping schemes. The difficulty of this scheme, however, is that this system is dynamically unstable. One solution is to use an additional optical field, at a different detuning, to stabilize the system. From Eqs. (4) and (5), taking  $\omega_e$ , we get

$$\frac{B}{K} = \frac{\hbar \frac{1}{1 + (\omega_e/\omega_0)^2} (\omega_e/\omega_0)^2}{1 + (\omega_e/\omega_0)^2 (\omega_e/\omega_0)^2 + 4(\omega_e/\omega_0)^2}; \quad (7)$$

suggesting that an optical field with larger detuning is less unstable for the same stiffness. The physical mechanism for this is that at larger detunings, the optical field resonates less strongly than for smaller detunings, so the time scale for the cavity response is shorter. To demonstrate this stabilization, consider that a carrier field (C) with detuning  $\omega_c - \omega_0 = 3$  creates a restoring force, but also a small anti-damping force. To counteract the anti-damping, a strong damping force is created by injecting a subcarrier (SC) with detuning  $\omega_{sc} - \omega_0 = 0.5$ . Because of its larger detuning, the C must have much higher incoming power than the SC for the restoring force of the C to dominate; we used a factor of 20. To illustrate the behavior of the system at all detunings, the various stability regions are shown in Figure 2. Point (d) in particular shows that the system is stable for our chosen parameters.

The experimental apparatus shown in Figure 1 was used to demonstrate several features of this proposal for optical trapping. We highlight four features important to this and future quantum measurements: (i) Extreme optical rigidity, allowing us to make an exceptionally stiff (but unstable) optical spring; (ii) Stabilization of the optical spring resonance by use of a second optical spring, allowing us to trap the mirror; (iii) Noise suppression, where the optical stiffness manifestly reduces the response of the mirror to external forces; and (iv) Optical cooling, where we determine the effective temperature of the stable optical spring mode to be well below room temperature.

Figure 3 shows the measured response functions of the optical spring for various input powers and detunings; they were measured either by applying a driving force to the input mirror, or by modulating the frequency of the laser light; both have the effect of modulating the cavity resonance condition.

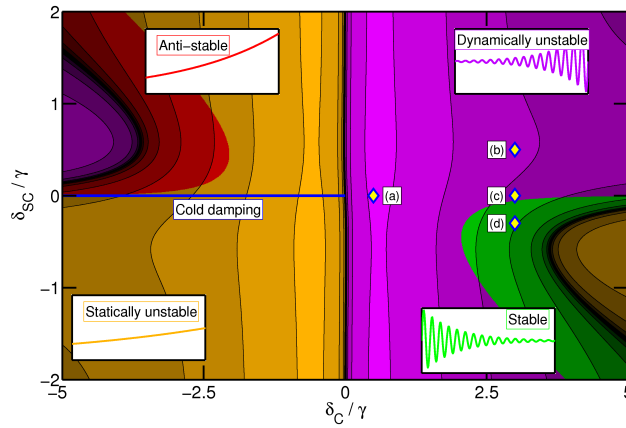


FIG. 2: Graphical representation of the total optical rigidity due to both optical fields, as a function of C and SC detuning, for fixed input power (power in the SC field is  $1=20$  the C power) and observation frequency ( $\omega = 2\pi \cdot 1$  kHz). The shaded regions correspond to detunings where the total spring constant  $K$  and damping constant  $\gamma$  are differently positive or negative, leading to stable or unstable equilibria. Specifically, "stable" corresponds to  $K > 0$ ;  $\gamma < 0$ , "anti-stable" to  $K < 0$ ;  $\gamma > 0$ , "statically unstable" to  $K < 0$ ;  $\gamma < 0$ , and "dynamically unstable" to  $K > 0$ ;  $\gamma > 0$ . The blue line denotes "cold damping" corresponding to  $\delta_c < 0$  and  $\delta_{sc} = 0$ , i.e., the SC provides no optical force. The (logarithmically spaced) contours shown are scaled according to  $K$ : brighter regions have larger  $K$ . The labels (a)–(d) refer to the measurements shown in Fig. 3.

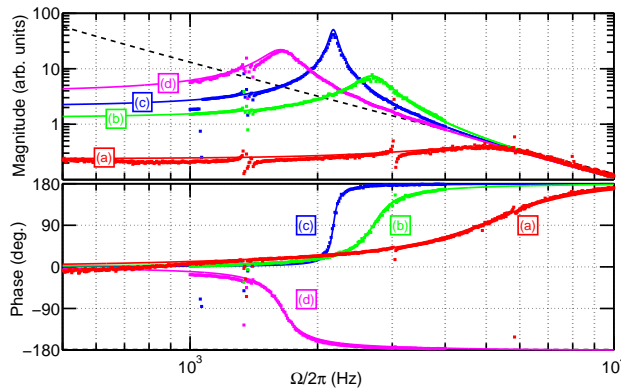


FIG. 3: The optical spring response for various power levels and detunings of the carrier and subcarrier. Measured transfer functions of displacement per force are shown as points, while the solid lines are theoretical curves. The dashed line shows the response of the system with no optical spring. An unstable optical spring resonance with varying damping and resonant frequency is produced when (a)  $\delta_c = 0.5$ ;  $\delta_{sc} = 0$ ; (b)  $\delta_c = 3$ ;  $\delta_{sc} = 0.5$ ; (c)  $\delta_c = 3$ ;  $\delta_{sc} = 0$ ; and it is stabilized in (d)  $\delta_c = 3$ ;  $\delta_{sc} = 0.3$ . Note that the damping of the optical spring increases greatly as the mechanical resonance frequency increases, approaching  $\omega_{mech}$  for the highest frequency optical spring.

(i) Extreme rigidity: With no SC detuning and  $\delta_c = 0.5$ , the 172 Hz mechanical resonance of the 1 gram mirror oscillator was shifted as high as 5 kHz (curve (a) in Fig. 3), corresponding to an optical rigidity of  $K = 2 \cdot 10^6$  N/m. To put this number into perspective, consider replacing the optical mode with a rigid beam with Young's modulus  $E$ . The effective Young's modulus of this mode with area  $A$  of the beam spot ( $0.6 \text{ mm}^2$ ) and length  $L = 0.9$  m of the cavity, is given by  $E = K L/A = 1.2$  TPa, stiffer than any known material (but also with very small breaking strength).

(ii) Stabilization: Also shown in Fig. 3 are curves corresponding to varying C and SC detunings. In curves (b), (c) and (d), we detune the C by more than the cavity linewidth since the optical spring is less unstable for large  $\delta_c$ . With  $\delta_c = 3$  and  $\delta_{sc} = 0$ , we reach  $\omega = 2\pi \cdot 2178$  Hz, shown in curve (c). Note that the optical spring is unstable, as evidenced by the phase increase of 180° about the resonance (corresponding to anti-damping). Next we detune the subcarrier, shown in curve (b) with  $\delta_{sc} = 0.5$ , which increases the resonant frequency and also increases the

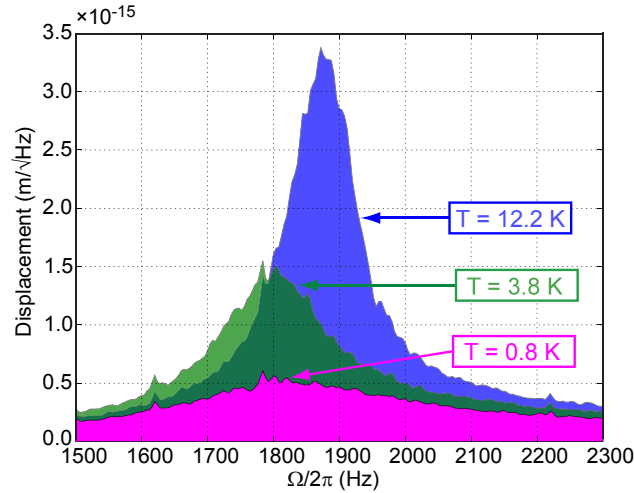


FIG. 4: The measured noise spectral density of the cavity length is shown for several configurations corresponding to different detunings. The magenta curve corresponds to  $c = 3$  and  $s_c = 0.5$ . The green and blue curves are obtained by reducing  $s_c$  and increasing  $c$  in order to keep  $\omega_e$  approximately constant, while varying  $\omega_c$ . The spectrum is integrated between 1500 and 2300 Hz to calculate the rms motion of the oscillator mode, giving effective temperatures of 0.8, 3.8 and 12.2 K. The limiting noise source here is not thermal noise, but in fact frequency noise of the laser, suggesting that with reduced frequency noise, even lower temperatures could be attained.

anti-damping, demonstrated by the broadening of the resonant peak. For these two cases, electronic servo control is used to keep the cavity locked. If the control system is disabled, then the cavity immediately loses lock. Remarkably, for  $s_c = 0.3$ , the optical spring resonance becomes stable, shown in curve (d), allowing operation of the cavity without electronic feedback at frequencies above 30 Hz; we note the change in phase behavior and the reduction of the resonant frequency. This is a powerful demonstration that we can precisely control the frequency and damping of the optical spring independently in the strong coupling regime.

(iii) Noise suppression: Additionally, we note that the response of the system at frequencies below the optical spring resonance is greatly reduced when compared to the natural response, by as much as  $10^3$ . This effect is of great importance to some quantum nondemolition experiments, such as in Ref. [18], which rely on this noise suppression effect to observe quantum effects.

(iv) Optical cooling: The noise in our experiment is presently dominated by frequency noise of the laser at  $\omega_c$ . We can nevertheless estimate the effective temperature of the optomechanical mode, as determined by this noise, according to Eq. (1). To determine  $x_{rms}$  in our experiment, we measure the noise spectral density of the error signal from the cavity, calibrated by injecting a frequency modulation of known amplitude at 12 kHz. The frequency fluctuation spectrum is converted into displacement noise by multiplying by  $L_0 = c$ . The displacement noise measured in this way is shown in Fig. 4; the shaded regions give  $x_{rms}$ , measured for different detunings, while attempting to keep  $\omega_e$  constant and changing only  $\omega_c$ . The lowest temperature demonstrated is 0.8 K.

In our experiment, we began with  $\omega_m = 2172$  Hz,  $\omega_m = \omega_m = 3200$ , and  $T = 295$  K, while the optical spring mode has  $\omega_e = 21800$  Hz,  $\omega_e = \omega_e = 6$ , and  $T_e = 0.8$  K. This corresponds to a factor of  $7.2 \times 10^7$  increase in  $N$ ; the error on this value comes from error estimates for measured values of temperature, as well as frequency and damping of the mode. We emphasize that standard cold damping cannot achieve this.

To explore the scope of the proposed technique, consider attempting to place a 1 gram oscillator in a low energy state. To reduce coupling to the environment, the mass is suspended with low suspension resonant frequency  $\omega_m = 21$  Hz, and to reduce thermal noise the mechanical damping is made as small as possible,  $\gamma_m = 10^{-6} \gamma_m$ . To cancel the effects of laser noise, two identical cavities can be placed in the arms of a Michelson interferometer. The laser light reflected from each cavity interferes destructively at the beam splitter, allowing for rejection of laser noise at the antisymmetric output. The laser frequency may be further locked to the common motion of the two arms, providing additional stabilization of laser frequency noise. The remaining differential motion of the arm cavity mirrors becomes the oscillator degree of freedom to be placed in a quantum state. This scheme is precisely the same as suggested in Ref. [18], and a detailed noise analysis is described there. It was proposed to use such a system to measure non-classical (squeezed) states of light that are created through coupling to the mirror position via radiation pressure, but

we show here that the same apparatus can also be used to approach the quantum ground state of the mirrors. Without optical trapping,  $N \approx 10^7$  for this system. At  $\omega = 2\pi \times 1$  kHz, thermal noise due to the dielectric coatings on the mirrors dominates, giving a noise spectral density of  $5 \times 10^{-19}$  m=Hz<sup>1/2</sup> (see Figure 3 of Ref. [18]). Assuming this is the limiting noise, and taking  $\epsilon = \epsilon_0 = 5$ , we find  $x_{rms} = 3.5 \times 10^{-17}$  m, which gives  $T_e = 3.5 \times 10^6$  K and  $N_e \approx 0.07$ . Reduction of this noise source by a further order of magnitude can be engineered by optimizing the aspect ratio of the mirror, and applying the best currently available mirror coatings whose mechanical loss is 50% lower than those assumed. We are, therefore, confident that technical and thermal noise do not preclude approaching the ground state, with  $N \approx 1$ , in such an apparatus. The ultimate limit of optical cooling comes from the vacuum noise of the optical fields. Consider the energy of a mode at frequency  $\omega_e$  whose displacement is limited by the standard quantum limit [2]

$$E = \frac{1}{2} M \omega_e^2 \left( \frac{8h}{M \omega_e^2} \right)^2 \frac{\omega_e^2}{\omega_e} = \frac{e}{4} \quad ; \quad (8)$$

The first term in parentheses is the optical spring constant  $K$ , the second term is the standard quantum limit (SQL) for displacement [2], the third term accounts for concentration of energy at the optical spring resonance, and the final term is due to integration over frequency rather than angular frequency. In the extreme case that  $\omega_e = \omega$ ,  $E = h \omega_e$ . It should be noted that in an SQL measurement, half of the inferred energy arises from detection noise, while the other half is produced by the radiation pressure forces. Since detection noise does not excite the mirror motion, the energy of the mirror is another factor of 2 lower, precisely the ground state energy of the oscillator. This result is supported by previous work [19], and suggests that this technique is suitable for approaching the ground state of gram-scale objects.

In conclusion, we have proposed a scheme that uses the optical spring effect to both reduce the occupation number and increase the lifetime of the mode of a mirror oscillator. We also provide an experimental demonstration that the technique is feasible, and show the path to observing quantum effects with large objects using present-day technologies.

We would like to thank our colleagues at the LIGO Laboratory and the MQM group, and also Steve Girvin; a casual discussion with Steve prompted some of the experimental work explored in this manuscript. We are also grateful to Mike Boyle for first prompting us to explore double optical springs, and to Kentaro Somiya for helpful discussions and introduction to the MQM group. We gratefully acknowledge support from National Science Foundation grants PHY-0107417 and PHY-0457264. Y.C.'s research was supported by the Alexander von Humboldt Foundation's Sofja Kovalevskaja Award (funded by the German Federal Ministry of Education and Research).

- 
- [1] C. H. Metzger and K. K. Arrai, *Nature* 432, 1002 (2004).  
 [2] V. Braginsky, Yu. Vorontsov, and K. Thorne, *Science* 209, 547 (1980).  
 [3] A. C. Almeida and A. Leggett, *Phys. Rev. A* 31, 1059 (1985).  
 [4] S. Mancini and P. Tombesi, *Phys. Rev. A* 49, 4055 (1994).  
 [5] D. Vitali, S. Mancini, and P. Tombesi, *Phys. Rev. A* 64, 051401(R) (2001).  
 [6] W. Marshall, C. Simon, R. Penrose, and D. Bouwmeester, *Phys. Rev. Lett.* 91, 130401 (2003).  
 [7] P. F. Cohadon, A. Heidmann, and M. P. Inard, *Phys. Rev. Lett.* 83, 3174 (1999).  
 [8] D. K. Leckner, W. Marshall, M. de Hood, K. Dinyari, B.-J. Pors, W. Irvine, and D. Bouwmeester, *Phys. Rev. Lett.* 96, 173901 (2006).  
 [9] T. Corbitt, D. Ottaway, E. Innerhofer, J. Pelc, and N. Mavalvala, *Phys. Rev. A* 74, 021802 (2006).  
 [10] A. N. Baik, O. Buu, M. D. LaHaye, A. D. Armour, A. A. Clerk, M. P. Blencowe, and K. C. Schwab, *Nature* 443, 193 (2006).  
 [11] S. Gigan, H. B. Ohm, M. Paternostro, F. B. Laser, G. Langer, J. Hertzberg, K. Schwab, D. Bauerle, M. Aspöckl, and A. Zeilinger, *Nature* 444, 67 (2006).  
 [12] D. K. Leckner and D. Bouwmeester, *Nature* 444, 75 (2006).  
 [13] O. Arcizet, P. F. Cohadon, T. Briant, M. P. Inard, and A. Heidmann, *Nature* 444, 71 (2006).  
 [14] A. Buonanno and Y. Chen, *Phys. Rev. D* 65, 042001 (2002).  
 [15] B. S. Sheard, M. B. Gray, C. M. Mow-Lowry, D. E. McClelland and S. E. Whitcomb, *Phys. Rev. A*, 69, 051801 (2004).  
 [16] O. Miyakawa, R. Ward, R. Adhikari, M. Evans, B. Abbott, R. Bork, D. Busby, J. Heefner, A. Ivanov, M. Smith, R. Taylor, S. Vass, A. Weinstein, M. Varvella, S. Kawamura, F. Kawazoe, S. Sakata, and C. Mow-Lowry, *Phys. Rev. D* 74, 022001 (2006).  
 [17] V. B. Braginsky and S. P. Vyatchanin, *Phys. Lett. A* 293, 228 (2002).  
 [18] T. Corbitt, Y. Chen, F. Khalili, D. Ottaway, S. Vyatchanin, S. Whitcomb and N. Mavalvala, *Phys. Rev. A* 73, 023801 (2006).  
 [19] V. Braginsky, M. G. Gorodetsky, F. Khalili, A. M. Atsko, K. Thorne, and S. Vyatchanin, *Phys. Rev. D* 67, 082001 (2003).